Rotational Line Broadening
Gray Chapter 18

Geometry and Doppler Shift
Profile as a Convolution
Rotational Broadening Function
Observed Stellar Rotation
Other Profile Shaping Processes

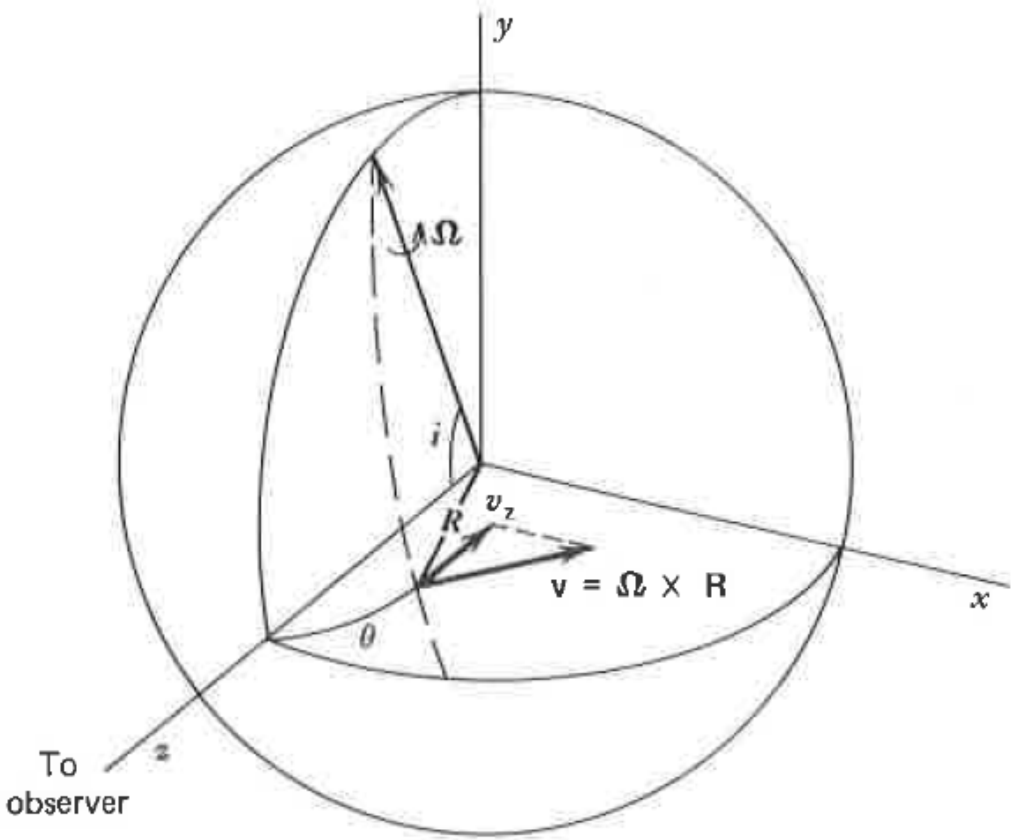

Fig. 17.2. The rotation axis is inclined at an angle i to the line of sight along the z axis. The y axis is chosen to make $\mathbf{\Omega}$ lie in the y–z plane. For some arbitrary point on the surface at an angle θ from the line of sight, the velocity is $\mathbf{\Omega} \times \boldsymbol{R}$, where $\boldsymbol{R}$ is the stellar radius. The z component of this velocity gives the Doppler shift.

Doppler Shift of Surface Element

- Assume spherical star with rigid body rotation
- Velocity at any point on visible hemisphere is

$$v = \Omega \times R$$

$$= \begin{vmatrix} \hat{x} & \hat{y} & \hat{z} \\ 0 & \Omega \sin i & \Omega \cos i \\ x & y & z \end{vmatrix} = \begin{array}{c} \left(z\Omega \sin i - y\Omega \cos i\right)\hat{x} \\ +\left(x\Omega \cos i\right)\hat{y} \\ +\left(-x\Omega \sin i\right)\hat{z} \end{array}$$

Doppler Shift of Surface Element

- z component corresponds to radial velocity
- Defined as positive for motion directed away from us (opposite of sense in diagram)
- Radial velocity is

$$v_R = x\Omega \sin i$$

- Doppler shift is

$$\Delta\lambda = \frac{\lambda_0}{c} v_R = \frac{\lambda_0}{c}\left(x\Omega \sin i\right)$$

Radial velocity depends only on x position. Largest at limb, x=R.

$$\Delta\lambda_L = \frac{\lambda_0}{c}\left(R\Omega\sin i\right) = \frac{\lambda_0}{c}\left(v\sin i\right)$$

v = equatorial rotational velocity,
$v \sin i$ = projected rotational velocity

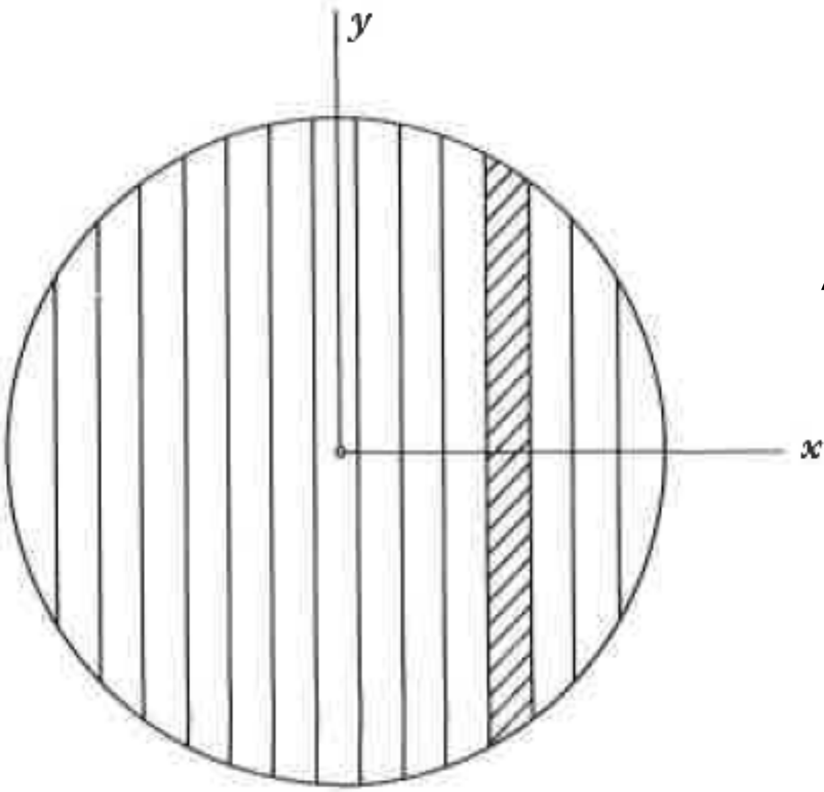

Fig. 17.3. The apparent disk of the star can be thought of as a series of strips, each having a Doppler shift according to eq. (17.1).

Flux Profile

- Observed flux is $(R/D)^2\ F_\nu$ where

$$F_\nu = \oint I_\nu \cos\theta \; d\omega$$

- Angular element for surface element dA

$$d\omega = {dA}/{R^2}$$

- Projected element

$$dx\ dy = dA \cos\theta$$

- Expression for flux

$$F_\nu = \iint \frac{I_\nu}{R^2}\, dx\ dy$$

Assumption: profile independent of position on visible hemisphere

$$F_\lambda = \iint H(\lambda - \Delta\lambda) I_c \, dx \, dy \, / R^2$$

$$= \int_{-R}^{+R} H(\lambda - \Delta\lambda) \int_{-y_1}^{+y_1} I_c \frac{dy}{R} \, d\left(\frac{\Delta\lambda}{\Delta\lambda_L}\right)$$

$$y_1 = \left(R^2 - x^2\right)^{1/2} = R\left[1 - \left(\frac{\Delta\lambda}{\Delta\lambda_L}\right)^2\right]^{1/2}$$

Express as a Convolution

$$G(\Delta\lambda) = \begin{cases} \dfrac{1}{\Delta\lambda_L} \dfrac{\int_{-y_1}^{+y_1} I_c \, dy / R}{\oint I_c \cos\theta \, d\omega} & for \; |\Delta\lambda| \leq \Delta\lambda_L \\ 0 & for \; |\Delta\lambda| > \Delta\lambda_L \end{cases}$$

$$\frac{F_\lambda}{F_c} = \int_{-R}^{+R} H(\lambda - \Delta\lambda) \, G(\Delta\lambda) = \int_{-\infty}^{+\infty} H(\lambda - \Delta\lambda) \, G(\Delta\lambda)$$

$$= H(\lambda) * G(\lambda)$$

$G(\lambda)$ for a Linear Limb Darkening Law

$$\frac{I_c}{I_c^0} = 1 - \varepsilon + \varepsilon \cos\theta$$

- Denominator of *G*

$$\oint I_c \cos\theta \, d\omega = \int_0^{\pi/2} \int_0^{2\pi} I_c \cos\theta \sin\theta \, d\theta \, d\phi \qquad \left(\mu = \cos\theta\right)$$

$$= -\int_1^0 \int_0^{2\pi} I_c \mu \, d\mu \, d\phi = 2\pi \int_0^1 I_c \mu \, d\mu$$

$$= 2\pi I_c^0 \int_0^1 (1-\varepsilon)\mu + \varepsilon\mu^2 \; d\mu = 2\pi I_c^0 \left[\frac{1-\varepsilon}{2} + \frac{\varepsilon}{3} \right]$$

$$= \pi I_c^0 \left[1 - \frac{\varepsilon}{3} \right]$$

$G(\lambda)$ for a Linear Limb Darkening Law

$$\frac{I_c}{I_c^0} = 1 - \varepsilon + \varepsilon\cos\theta$$

- Numerator of *G*

$$\int_{-y_1}^{+y_1} I_c \frac{dy}{R} = 2I_c^0 \int_0^{y_1} 2I_c^0 \left[\left(1-\varepsilon\right) + \varepsilon\cos\theta\right]\frac{dy}{R}$$

$$= 2I_c^0\left(1-\varepsilon\right)\frac{y_1}{R} + 2\varepsilon I_c^0 \int_0^{y_1} \cos\theta \frac{dy}{R}$$

$$= 2I_c^0\left(1-\varepsilon\right)\left[1-\left(\frac{\Delta\lambda}{\Delta\lambda_L}\right)^2\right]^{1/2} + 2\varepsilon I_c^0 \int_0^{y_1} \frac{1}{R^2}\sqrt{R^2 - x^2 - y^2}\, dy$$

G(λ) for a Linear Limb Darkening Law

$$\frac{I_c}{I_c^0} = 1 - \varepsilon + \varepsilon \cos\theta$$

- Analytical solution for second term in numerator

$$\int \left(A^2 - y^2\right)^{1/2} dy = \frac{1}{2}\left[y\left(A^2 - y^2\right)^{1/2} + A^2 \arcsin\frac{y}{|A|}\right]$$

- Second term is

$$2\varepsilon I_c^0 \frac{1}{2}\frac{1}{R^2}\left[y(R^2 - x^2 - y^2)^{1/2} + (R^2 - x^2)\arcsin\frac{y}{\sqrt{R^2 - x^2}}\right]_0^{y_1}$$

$$= \frac{\varepsilon I_c^0}{R^2}\left[(R^2 - x^2)\frac{\pi}{2}\right] \qquad \left(y_1 = \sqrt{R^2 - x^2}\right)$$

$$= \frac{\pi}{2}\varepsilon I_c^0\left[1 - \left(\frac{\Delta\lambda}{\Delta\lambda_L}\right)^2\right]$$

G(λ) for a Linear Limb Darkening Law

$$\frac{I_c}{I_c^0} = 1 - \varepsilon + \varepsilon \cos\theta$$

$$\therefore G(\Delta\lambda) = \frac{2(1-\varepsilon)\left[1-\left(\frac{\Delta\lambda}{\Delta\lambda_L}\right)^2\right]^{1/2} + \frac{\pi}{2}\varepsilon\left[1-\left(\frac{\Delta\lambda}{\Delta\lambda_L}\right)^2\right]}{\pi\Delta\lambda_L\left(1-\frac{\varepsilon}{3}\right)}$$

$$= c_1\underbrace{\left[1-\left(\frac{\Delta\lambda}{\Delta\lambda_L}\right)^2\right]^{1/2}}_{\Uparrow \text{ ellipse}} + c_2\underbrace{\left[1-\left(\frac{\Delta\lambda}{\Delta\lambda_L}\right)^2\right]}_{\Uparrow \text{ parabola}}$$

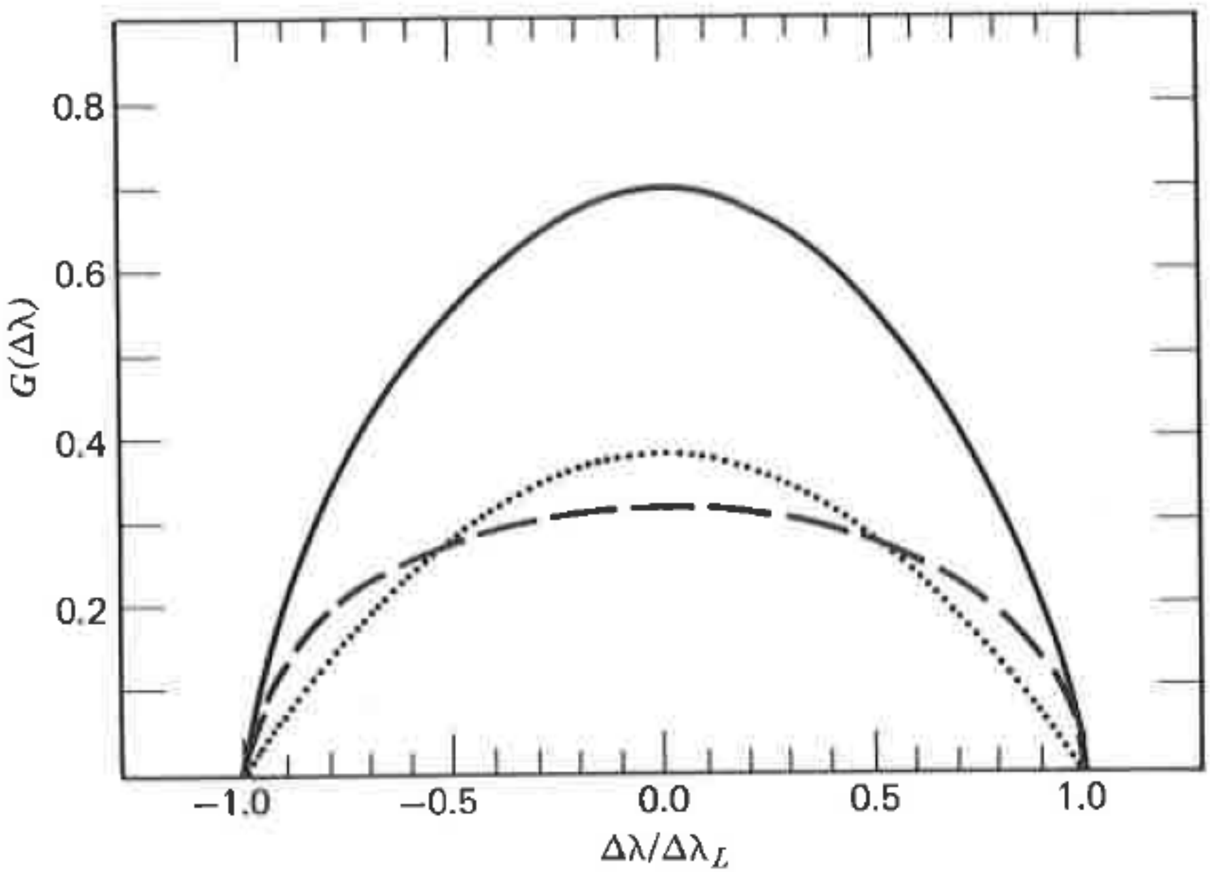

Fig. 17.5. The rotation profile, according to eq. (17.12), is shown by the top-most line for $\varepsilon = 0.6$. The first term (no limb darkening) is shown as the dashed curve; the second term as the dotted curve.

Grey atmosphere case: $\varepsilon = 0.6$

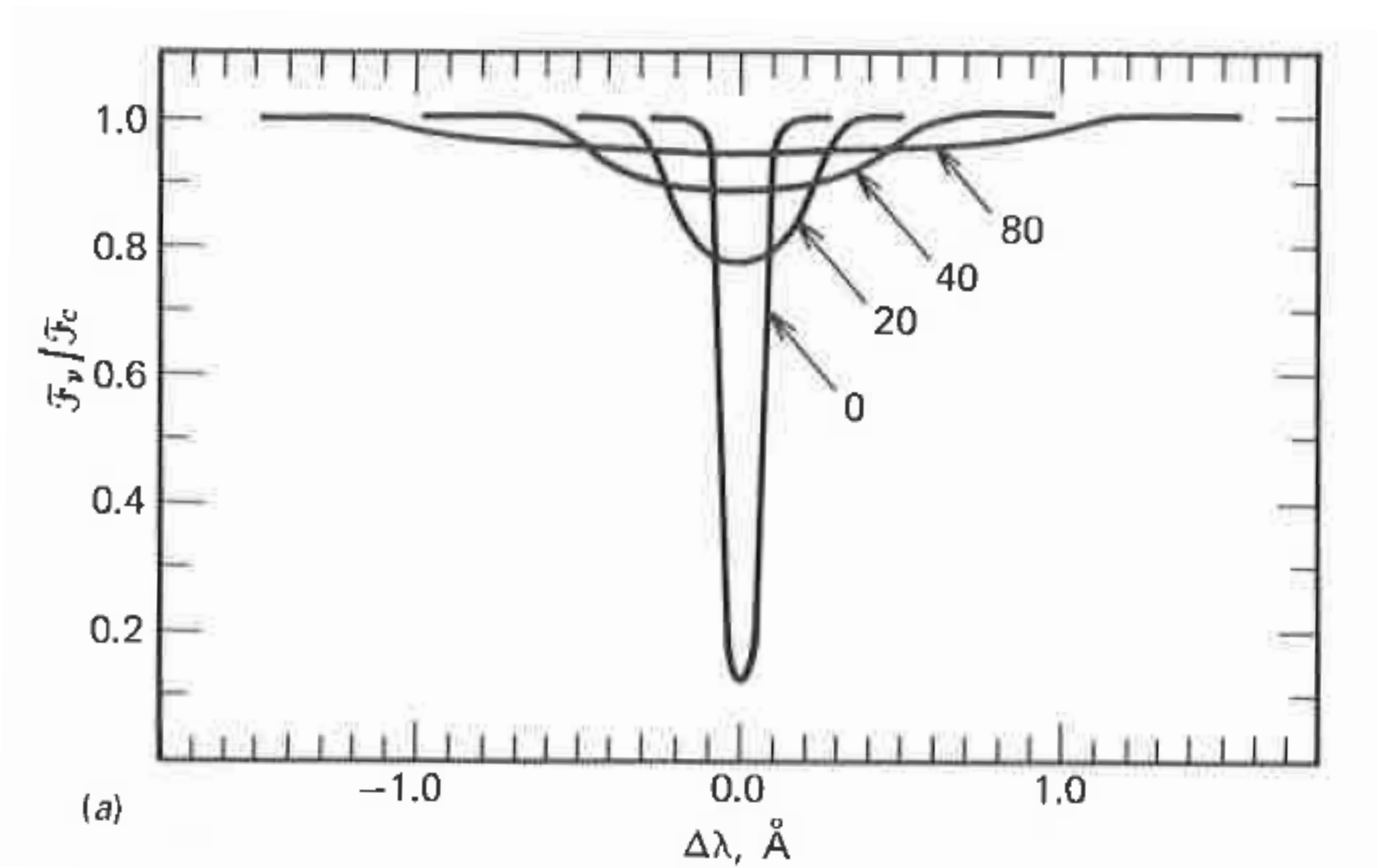
1.0
0.8
0.6
0.4
0.2
80
40
20
0
−1.0
0.0
1.0
(a)
Δλ, Å

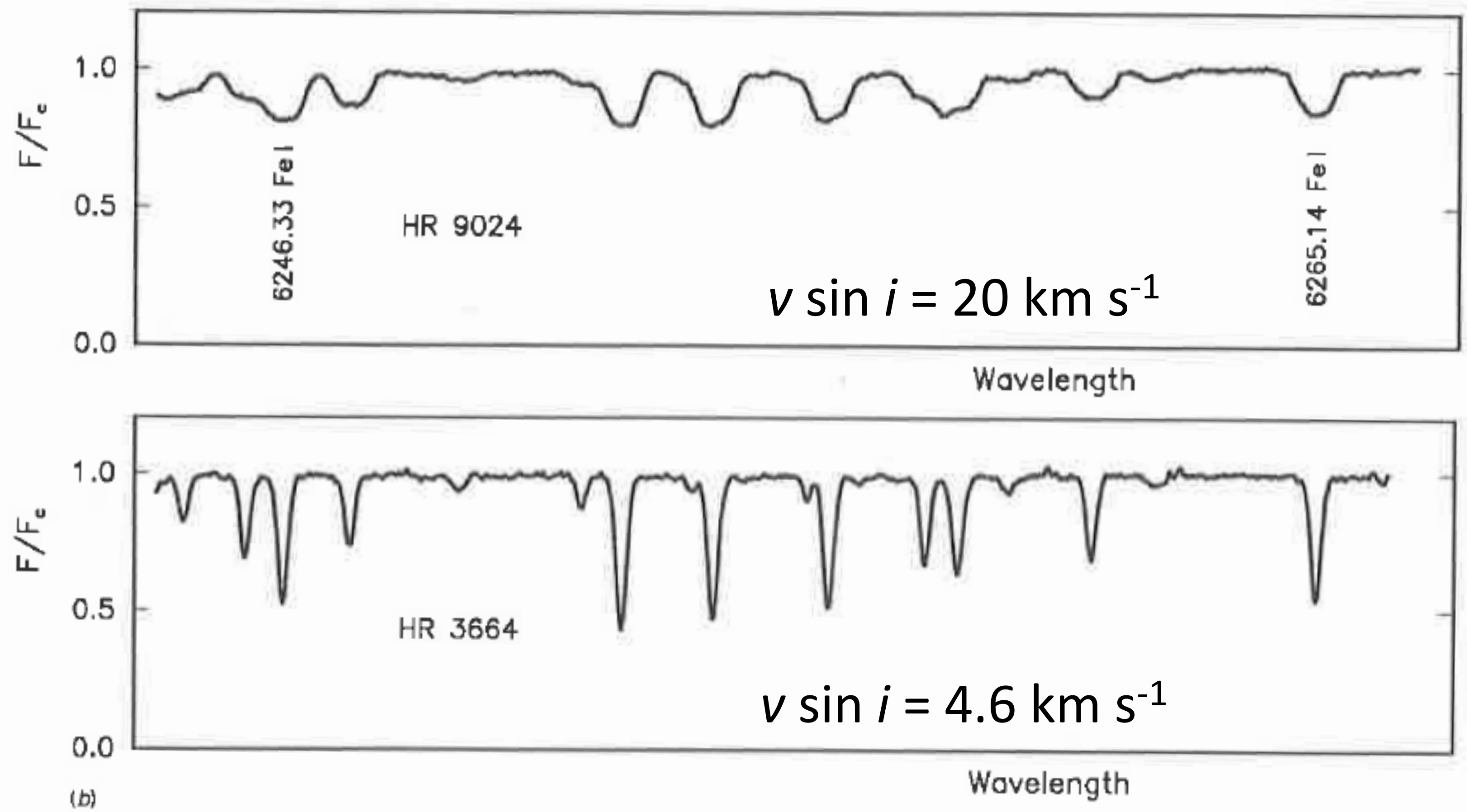

Fig. 17.7. (*a*) Computed profiles illustrate the broadening effect of rotation. The profiles are labeled with $v \sin i$. the wavelength is 4243 Å, and the line has an equivalent width of 100 mÅ. (*b*) These two early-G giants illustrate the Doppler broadening of the line profiles by rotation.

Measurement of Rotation

- Use intrinsically narrow lines
- Possible to calibrate half width with $v \sin i$, but this will become invalid in very fast rotators that become oblate and gravity darkened
- Gray shows that $G(\Delta\lambda)$ has a distinctive appearance in the Fourier domain, so that zeros of FT are related to $v \sin i$
- Rotation period can be determined for stars with spots and/or active chromospheres by measuring transit times

Rotation in Main Sequence Stars

- massive stars rotate quickly with rapid decline in F-stars (convection begins)
- low mass stars have early, rapid spin down, followed by weak breaking due to magnetism and winds (gyrochronology)

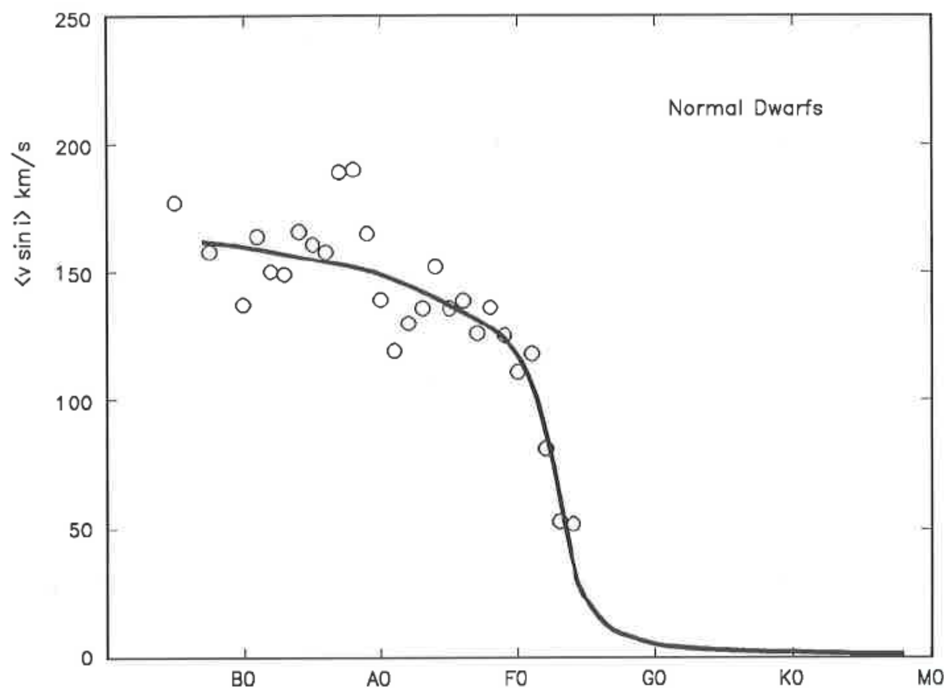

Fig. 17.16. The average rotation rates are shown for spectral intervals as a function of spectral type. (Data are from Uesugi and Fukuda (1982), Soderblom (1983), and Gray (1982b, 1984b).)

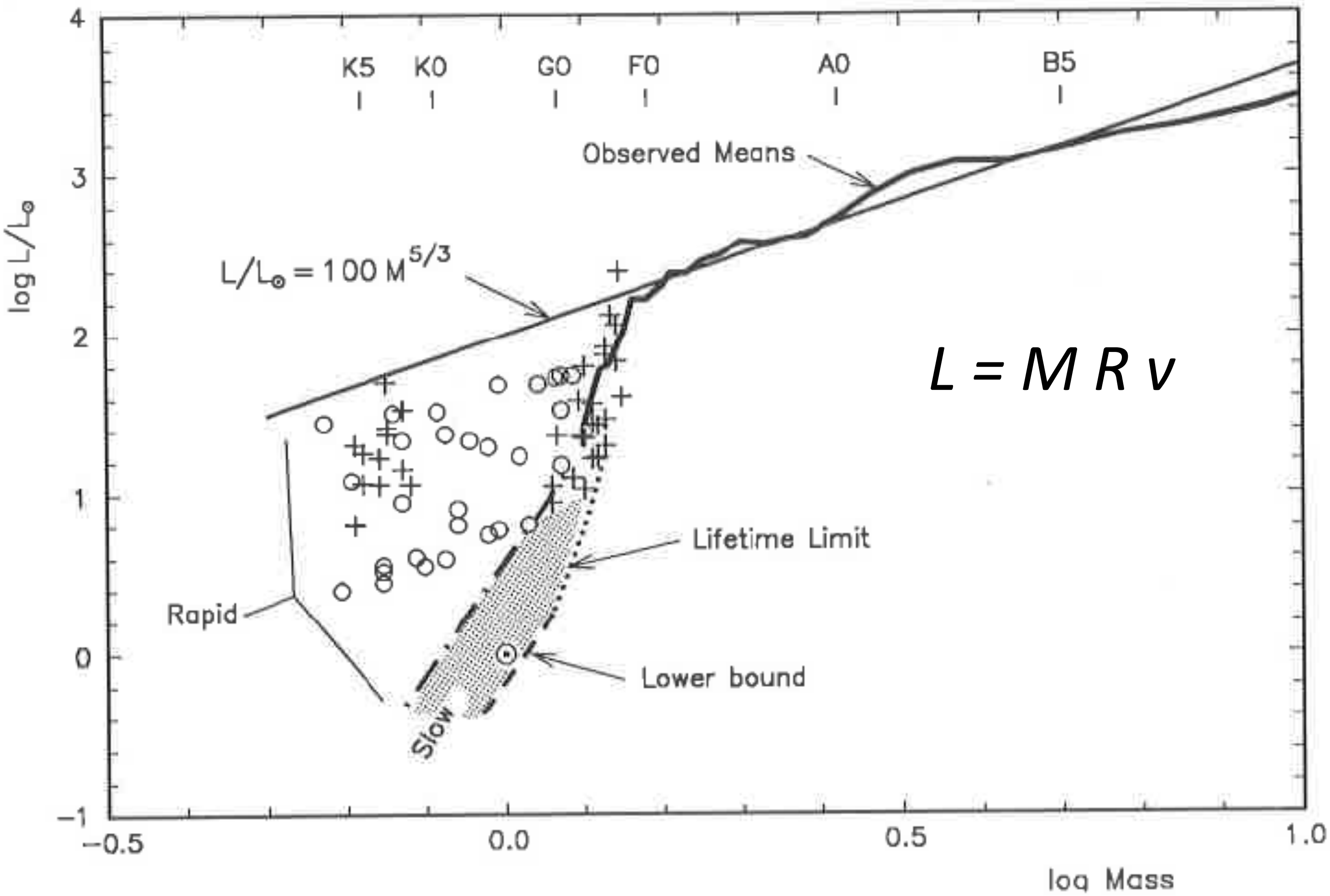

$L = M\, R\, v$

Fig. 17.18. Here pseudo-angular momentum (L = mass × radius × equatorial rotation rate) for dwarfs is shown as a function of mass. The stars earlier than about F2 delineate a relation in which L varies as the $\frac{5}{3}$ power of the mass. The rapid-braking domain and the slow-braking domains are indicated. Most dwarfs, including the sun (⊙), are found in the slow-braking region. Cooler Pleiades (+) and α Per-cluster stars (○) are seen in the rapid-braking phase.

Angular Momentum – Mass Relation

- Equilibrium with gravity = centripetal acceleration

$$\frac{GM}{R^2} = \frac{v^2}{R} \Rightarrow \frac{GM}{R^3} = \frac{v^2}{R^2} = \omega^2 \Rightarrow \omega \propto \sqrt{\rho}$$

- Angular momentum for uniform density

$$L = MRv = MR^2\omega \qquad \left(L = I\omega = k^2 MR^2\omega\right)$$

- In terms of angular speed and density

$$R^3 = \frac{GM}{\omega^2} \Rightarrow R = \left(\frac{GM}{\omega^2}\right)^{1/3}$$

$$L \propto M\, M^{2/3}\omega^{-4/3}\omega = M^{5/3}\omega^{-1/3} \propto M^{5/3}\rho^{-1/6}$$

- Density varies slowly along main sequence $L \propto M^{5/3}$

Rotation in Evolved Stars

- conserve angular momentum, so as *R* increases, *v* decreases
- Magnetic breaking continues (as long as magnetic field exists)
- Tides in close binary systems lead to synchronous rotation

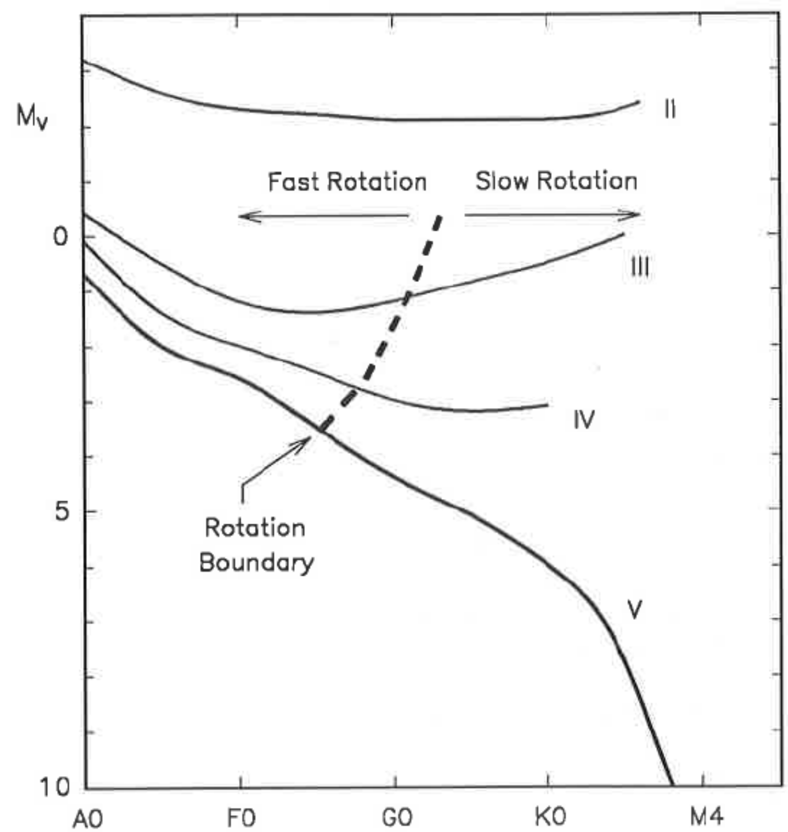

Fig. 17.21. The rotation boundary separates fast rotation from slow rotation.

Fastest Rotators

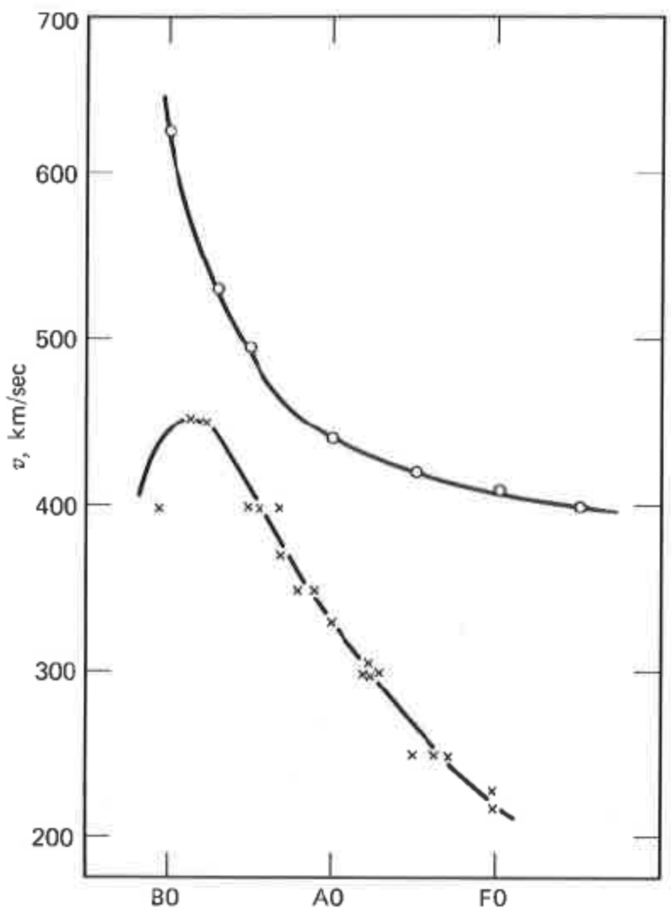

Fig. 17.22. The fastest rotation rates are shown by the ×s. The theoretical break-up velocities (top curve) approach the observed relation most closely in the B-star range. (Data from Slettebak (1966).)

- Critical rotation

$$v_{crit} = \sqrt{\frac{GM}{R}} = 437 \left(\frac{M/M_{sun}}{R/R_{sun}} \right)^{1/2} km\ s^{-1}$$

- Closest to critical in the B stars where we find Be stars (with disks)
- Spun up by Roche lobe overflow from former mass donor in some cases (ϕ Persei)

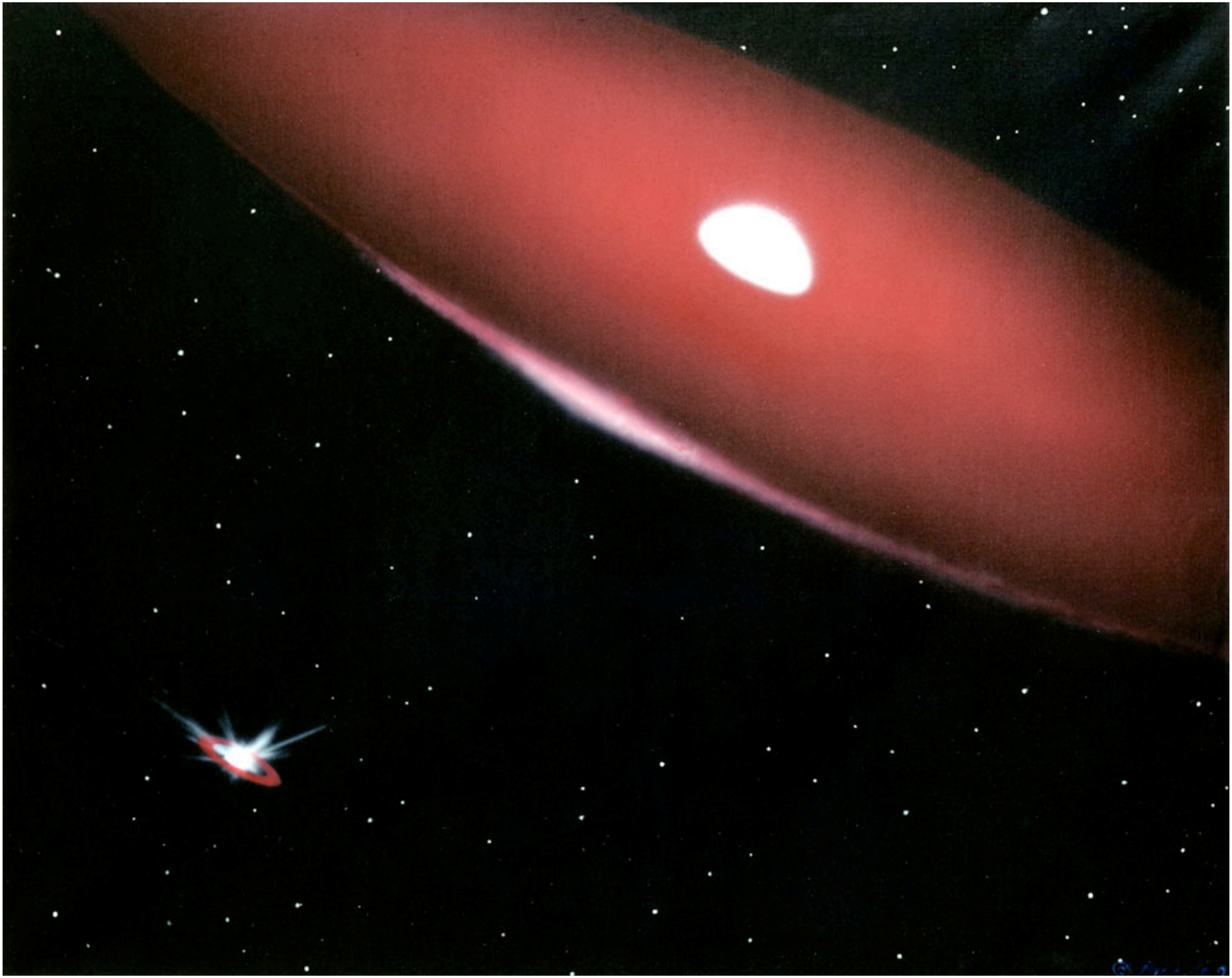

Other Processes That Shape Lines

- Macroturbulence and granulation http://astro.uwo.ca/~dfgray/Granulation.html

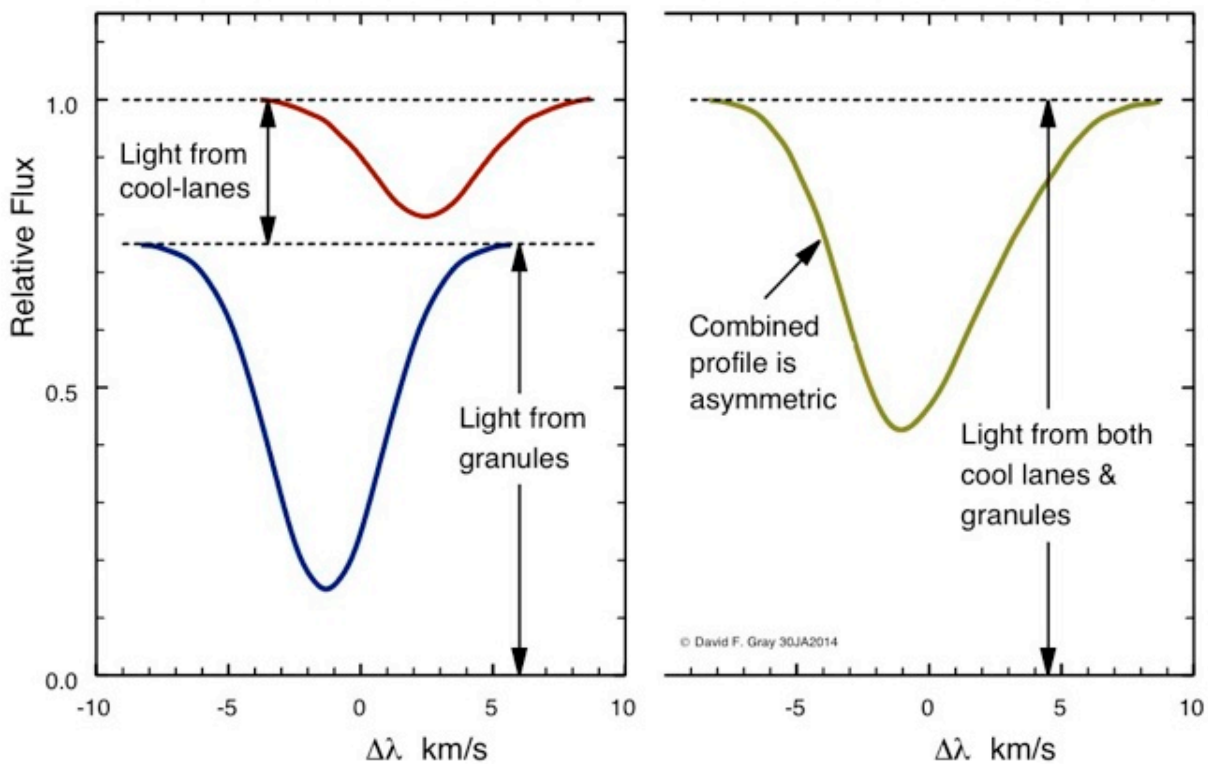

Star Spots

Vogt & Penrod 1983, ApJ, 275, 661

HR 3831
Kochukhov et al. 2004, A&A, 424, 935
http://www.astro.uu.se/~oleg/research.html

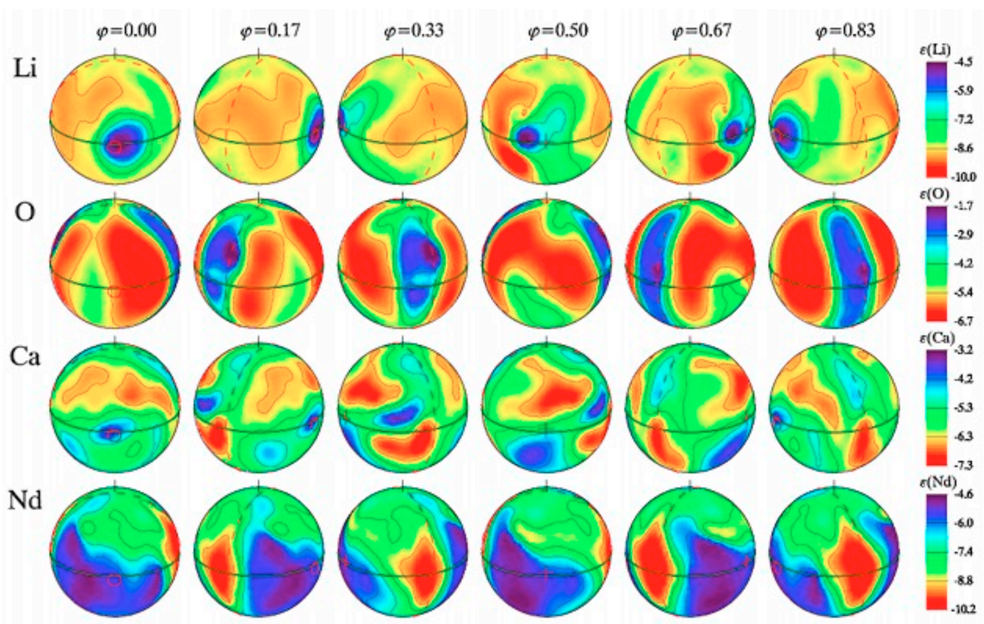

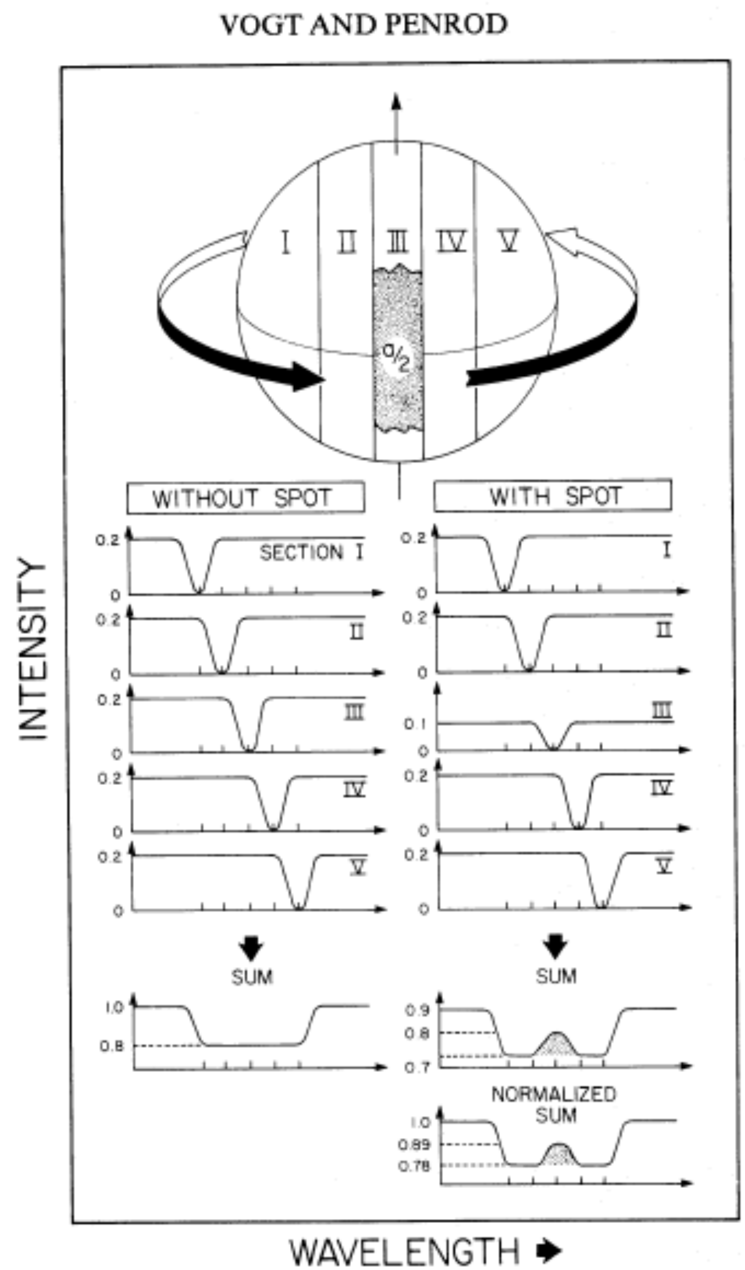

Stellar Pulsation

http://staff.not.iac.es/~jht/science/

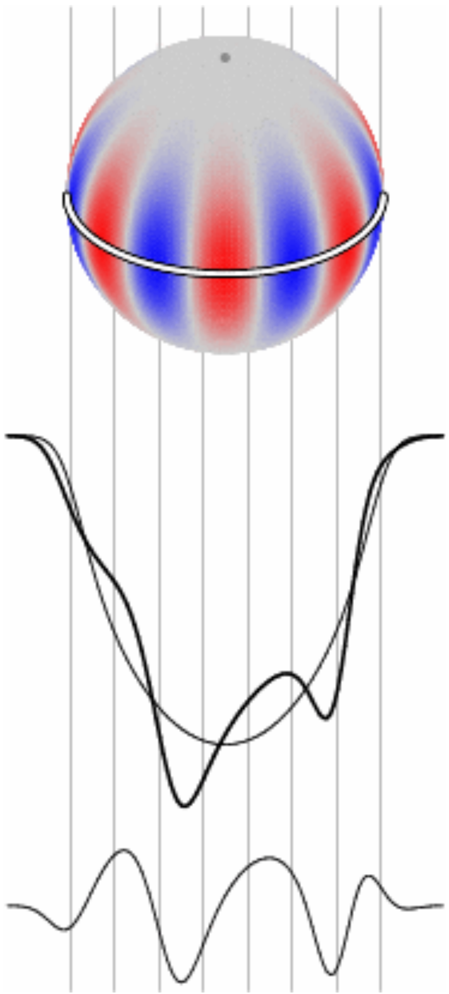

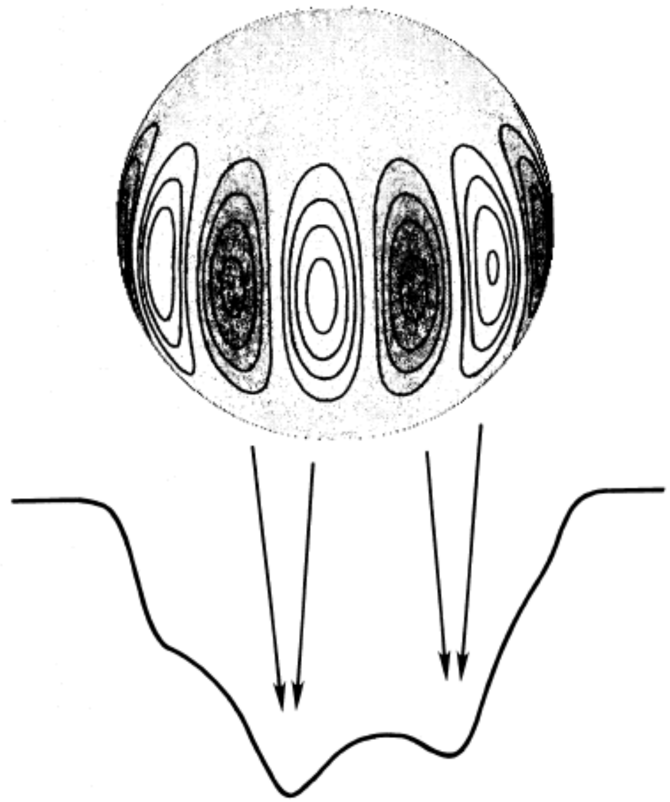

FIG. 16.—Illustration of the formation of distortions in the line profiles of a rapidly rotating nonradially oscillating star. This is a velocity map of the star with the resultant line profile shown below. The width of the line profile has been scaled to match the diameter of the star, thus reflecting the mapping which occurs between position across the disk and position across the line profile. The darkest shaded regions correspond to material moving away from the observer, while the lightest regions represent material moving toward the observer. Contours are drawn every 5 km s^{-1}.

Vogt & Penrod 1983, ApJ, 275, 661